



HAL
open science

Self-Assembled Micelles Prepared From Amphiphilic Dextran-Polylactide Diblock Copolymers for Antitumor Drug Release

Haozhi Sun, Shuxin Wang, Yuandou Wang, Linlin Lu, Feng Su, Suming Li

► **To cite this version:**

Haozhi Sun, Shuxin Wang, Yuandou Wang, Linlin Lu, Feng Su, et al.. Self-Assembled Micelles Prepared From Amphiphilic Dextran-Polylactide Diblock Copolymers for Antitumor Drug Release. *Polymers for Advanced Technologies*, 2025, 36 (4), <10.1002/pat.70162>. <hal-05370452>

HAL Id: hal-05370452

<https://hal.umontpellier.fr/hal-05370452v1>

Submitted on 20 Jan 2026

HAL is a multi-disciplinary open access archive for the deposit and dissemination of scientific research documents, whether they are published or not. The documents may come from teaching and research institutions in France or abroad, or from public or private research centers.

L'archive ouverte pluridisciplinaire **HAL**, est destinée au dépôt et à la diffusion de documents scientifiques de niveau recherche, publiés ou non, émanant des établissements d'enseignement et de recherche français ou étrangers, des laboratoires publics ou privés.



HAL Authorization

1 **Self-assembled micelles prepared from amphiphilic dextran-**
2 **polylactide diblock copolymers for anti-tumor drug release**

3
4 Haozhi Sun,¹ Shuxin Wang,¹ Yuandou Wang,¹ Linlin Lu,^{2*} Feng Su,^{1*} Suming Li ^{3*}

5
6 ¹ College of Chemical Engineering, Qingdao University of Science and Technology, Qingdao,
7 China

8 ² Qingdao Cancer Prevention and Treatment Research Institute, Qingdao Central Hospital,
9 University of Health and Rehabilitation Sciences (Qingdao Central Hospital), Qingdao, China

10 ³ Institut Européen des Membranes, IEM UMR 5635, Univ Montpellier, CNRS, ENSCM,
11 Montpellier, France

12
13 * Correspondence:

14 Linlin Lu, Qingdao Cancer Prevention and Treatment Research Institute, Qingdao Central
15 Hospital, University of Health and Rehabilitation Sciences, Qingdao, China

16 Email : lulinlin2007@hotmail.com.

17 Feng Su, College of Chemical Engineering, Qingdao University of Science and
18 Technology, Qingdao 266042, China.

19 Email: sufeng@qust.edu.cn

20 Suming Li, Institute Européen des Membranes, IEM, UMR 5635, Univ Montpellier,
21 CNRS, ENSCM, 34095 Montpellier, France.

22 Email: suming.li@umontpellier.fr
23
24

25 **ABSTRACT**

26 Fully biobased diblock copolymers were synthesized by reducing amination
27 from dextran (DEX) and amino terminated polylactide (PLA). The resulted copolymers
28 were characterized by using nuclear magnetic resonance, Fourier-transform infrared
29 spectroscopy, gel permeation chromatography, and Kaiser test. Self-assembled
30 copolymer micelles were characterized by transmission electron microscopy and
31 dynamic light scattering. The micelles are spherical in shape, and the particle size
32 increases with increase of both DEX and PLA block length. The critical micellar
33 concentration (CMC) of copolymers was determined by fluorescence spectrometry.
34 Data showed that the CMC decreases with increase of PLA block length. Drug loading
35 and drug release properties of DEX-PLA micelles were evaluated using curcumin as
36 model drug. An increase in drug loading content is obtained with increase of the PLA
37 block length. In vitro drug release from DEX-PLA micelles was performed at 37°C in
38 phosphate buffered saline. Biphasic release was observed with an initial burst followed
39 by slower release. The drug release rate from DEX-PLA micelles was mainly related to
40 copolymer composition, and reached 84.17% at 120 h for the copolymer with the
41 highest hydrophilic/hydrophobic ratio (DEX_{10K}-PLA₂₀). DEX-PLA micelles present
42 good cytocompatibility as evidenced by MTT assay, and drug loaded micelles exhibit
43 significant cytotoxicity to HeLa cells. The half maximum inhibitory concentration (IC₅₀)
44 of drug loaded DEX_{10K}-PLA₂₀ micelles was 9.12 µg/mL, which was lower than that of
45 free curcumin (11.9 µg/mL). Therefore, self-assembled micelles prepared from fully
46 biobased DEX-PLA copolymers could be a promising nanocarrier for hydrophobic
47 antitumor drugs.

48 **Keywords** : Dextran; polylactide; self-assembly; amphiphilic block copolymer;
49 micelle; drug release

50

51

52

53

54

55

56

57 **1. Introduction**

58 Amphiphilic block copolymers can spontaneously self-assemble in water to form
59 nano-size micelles composed of a hydrophilic shell and a lipophilic core.¹ The
60 hydrophilic segments form the outer layer of micelles, which allows to maintain the
61 structural stability, and prolong the blood circulation time.^{2, 3} On the other hand, the
62 hydrophobic segments form a solid core of micelles which serves as reservoir for drug
63 loading through physical or electrostatic interactions.^{4,5} In the past decades, polymeric
64 micelles have attracted more and more attention as nanocarrier in the field of controlled
65 drug release due to their good stability, high drug loading, improved bioavailability of
66 drugs, and reduced side effects.⁶⁻¹⁰

67 Poly(lactic acid) or polylactide (PLA) is a biobased polymer with outstanding
68 biodegradability and biocompatibility. PLA has been widely investigated for
69 applications in food packaging, mulch film in agriculture, medical implants, drug
70 carrier, etc.¹¹⁻¹⁵ When PLA is used as a drug carrier, drug release is generally controlled
71 by drug diffusion and polymer degradation. PLA is also used as a hydrophobic block to
72 build amphiphilic block copolymers with many hydrophilic polymers such as
73 poly(ethylene glycol) (PEG),¹⁶⁻¹⁸ poly(2-ethyl-2-oxazoline) (PEtOx),¹⁹ poly(N-
74 isopropylacrylamide) (PNIPAAm),²⁰ etc. The resulting copolymers, and in particular
75 PLA-PEG, present great interest as drug carrier in the form of self-assembled micelles.
76 Nevertheless, the widespread use of PEG in drug delivery systems is limited by its
77 immunogenicity, particularly the induction of anti-PEG antibodies which accelerate the
78 clearance of PEGylated systems.²¹

79 Polysaccharides such as cellulose, chitosan, alginate and dextran, are biopolymers
80 derived from renewable resources, including plants, seaweeds, microorganisms and
81 crustacean wastes. They are largely used as biomaterials due to their excellent
82 biocompatibility, non-toxicity; hydrophilicity and biodegradability.²²⁻²⁴

83 Polysaccharides are also used as a hydrophilic block to build amphiphilic block
84 copolymers with hydrophobic polymers. Recently, Lu et al. synthesized a series of
85 amphiphilic block copolymers by reductive amination between the hemiacetal reducing
86 end of hydroxypropyl methyl cellulose (HPMC) and the amine terminal group of
87 Jeffamine,²⁵ amino terminated PLA,²⁶ and amino terminated poly(ϵ -caprolactone)
88 (PCL).²⁷ The resulted copolymers are able to self-assemble into spherical micelles in
89 aqueous medium, showing great potential as nanocarrier of hydrophobic drugs.

90 Dextran is a bacterial polysaccharide composed of a main chain of α -1,6-linked
91 glucose and α -1,3 branches with a large number of hydroxyl groups. Dextran has been
92 used to conceive drug carriers in the form of conjugates, nanoparticles, and hydrogels.²⁸
93 Both PLA and DEX are biobased materials with good biocompatibility. Amphiphilic
94 block polymers have been synthesized from PLA and DEX for the preparation of drug
95 release systems. Verma et al. synthesized DEX-PLA block copolymer in three steps: (1)
96 reductive amination between dextran and N-Boc-ethylenediamine, (2) removal of the
97 Boc group, and (3) conjugation of amino terminated dextran and carboxy-terminated
98 PLA in the presence of N-(3-dimethylaminopropyl)-N'-ethylcarbodiimide (EDC) and
99 N-hydroxysulfosuccinimide (NHS).²⁹ On the other hand, in the work of Wang et al.,³⁰
100 DEX was end modified by reaction with ethylenediamine, and PLA was modified with
101 acryloyl chloride. Finally, DEX-PLA amphiphilic diblock copolymer was synthesized
102 by coupling of amino-terminated dextran and acryloyl-terminated PLLA via Michael
103 addition reaction. In both cases, excess DEX was used, and the reaction process was
104 complex and tedious.

105 Curcumin is a natural polyphenol derived from *curcuma longa*. It exhibits a wide
106 spectrum of pharmacological activities including anti-oxidant, anti-inflammatory, anti-
107 microbial, and anti-amyloid properties. Importantly, curcumin presents an effective
108 therapeutic effect on cancers such as breast cancer, lung cancer and blood tumors due
109 to its diverse range of molecular targets.^{31,32} Nevertheless, the therapeutic efficacy of
110 curcumin is limited by its extremely low water solubility, rapid metabolism, and low
111 bioavailability. Nanotechnology based drug delivery systems have been developed to
112 enhance the therapeutic efficacy of curcumin, including nanoparticles, liposomes and

113 phospholipids.³³

114 In this work, DEX-PLA copolymers with different DEX and PLA chain lengths
115 were synthesized by reductive amination between the amino group of NH₂-PLA and
116 the hemiacetal end group of DEX according to the synthesis method reported by Lu et
117 al.²⁶ The size and morphology, zeta potential and critical micelle concentration of self-
118 assembled micelles were determined. The drug loading and release capacity of the
119 micelles was studied using curcumin as a drug model. Finally the cytocompatibility of
120 blank micelles and the antitumor activity of drug loaded micelles were studied to
121 evaluate their potential as drug carrier in cancer treatment.

122

123 **2. Materials and methods**

124 **2.1. Materials**

125 Sodium triacetoxyborohydride (NaBH(OAc)₃), DEX with molecular weight of
126 5000 and 10000, trifluoroacetic acid (TFA), EDC, NHS and curcumin were obtained
127 from Shanghai Macklin Biochemical Co., Ltd. (Shanghai, China). L-lactide and DL-
128 lactide were purchased from Daigang Biotechnology Co., Ltd. (Shandong, China) and
129 purified by recrystallization in ethyl acetate. Tert-butyl-N-(3-hydroxypropyl)
130 carbamate (3-(Boc-amino)-1-propanol) was obtained from Sahn Chemical Technology
131 Co. Ltd. (Shanghai, China). Tin (II) 2-ethyl hexanoate (Sn(Oct)₂) purchased from Alfa
132 Aesar Co., Ltd. (Shanghai, China). Toluene and dichloromethane were obtained from
133 Sigma-Aldrich, dried over by calcium chloride (CaCl₂) and distilled prior to use. Mouse
134 fibroblasts L-929 cells and HeLa cells were provided by Qilu Stem Cell Engineering
135 Co., Ltd. (Shandong, China). Dulbecco's modified Eagle medium (DMEM), fetal
136 bovine serum (FBS) and other reagents were purchased from Beijing Solarbio Science
137 & Technology Co., Ltd. (Beijing, China). All other reagents were of analytic grade from
138 Sigma-Aldrich and used without further purification.

139 **2.2. Synthesis of amino-terminated PLA**

140 Amino-terminated PLA was synthesized by ring-opening polymerization of
141 lactide using 3-(Boc-amino)-1-propanol as initiator and Sn(Oct)₂ as catalyst, followed

142 by removal of Boc protective group under the action of TFA.²⁶ Typically, L-lactide
143 (2.592 g, 18 mmol), D, L-lactide (0.288 g, 2 mmol), 3-(Boc-amino)-1-propanol (0.35
144 g, 2 mmol), and Sn(Oct)₂ (0.0932 g, 0.23 mmol) were added to a three-mouth flask. 20
145 mL anhydrous toluene was added under N₂ atmosphere, and the solution was degassed
146 through five freeze-pump-thawing cycles. Then, the reaction proceeded at 80 °C for 24
147 h. BOC-NH-PLA was then obtained by precipitation with ethanol, followed by
148 centrifugation and vacuum drying.

149 In a flask under N₂ purge, 1.0 g BOC-NH-PLA was dissolved in 5 mL freshly
150 distilled dichloromethane. 5 mL anhydrous TFA was then added, and the reaction
151 proceeded for 1 h at room temperature. The crude product was obtained after removal
152 of all the liquid. It was then dissolved in dichloromethane, successively washed with 5%
153 NaHCO₃ aqueous solution and distilled water, dried with MgSO₄. Finally the solution
154 was filtrated, precipitated in cold ethanol, and vacuum dried up to constant weight to
155 yield NH₂-PLA.

156 **2.3. Synthesis of DEX-PLA block copolymer**

157 Six DEX-PLA block copolymers were synthesized by reduction amination from
158 dextran with molar mass of 5000 and 10000 and PLA with degree of polymerization
159 (DP) of 20, 30 and 40, respectively.^{26, 34} Typically, under N₂ atmosphere, DEX_{10k} (0.5
160 g, 0.05 mmol), NH₂-PLA (0.3 g, 0.05 mmol) and NaBH(OAc)₃ (0.042 g, 0.2 mmol)
161 were dissolved in 20 mL anhydrous DMSO. The reaction proceeded at 35 °C under N₂
162 atmosphere for 72 h. The solution was then dialyzed against distilled water for 72 h,
163 and freeze-dried to obtain the final product.

164 **2.4. Characterization**

165 A Bruker AVANCE 500 spectrometer with an operating frequency of 500 MHz
166 was used for nuclear magnetic resonance (NMR) analysis with tetramethylsilane as
167 internal reference and CDCl₃, DMSO or D₂O as solvent.

168 Gel permeation chromatography (GPC) was performed on a Shimadzu instrument
169 equipped with a Waters 410 refractive index detector. Polystyrene standards were used
170 for calibration, and tetrahydrofuran (THF) as the mobile phase. Samples at a

171 concentration of 5 mg/mL were filtered through a PTFE filter of 0.22 μm before
172 analysis at a flow rate of 1.0 mL/min.

173 Fourier transform infrared spectroscopy (FT-IR) was realized on TENSOR 27 FT-
174 IR spectrometer (Bruker Optics, Germany). Samples were prepared using potassium
175 bromide (KBr) pellet method. 32 scans were made for each measurement in the
176 wavenumber range of 400 - 4000 cm^{-1} .

177 Kaiser test was performed to detect the presence of primary amine from color
178 changes,³⁵⁻³⁷ using three color development agents, i.e. ethanol solution containing 6%
179 ninhydrin (reagent A), ethanol solution containing 80% phenol (reagent B) and pyridine
180 solution containing 2% 0.001M KCN (reagent C). A small amount of polymer was
181 added into a test tube, followed by addition of 2-3 drops of the above reagents A, B and
182 C. The mixture was heated at 110 $^{\circ}\text{C}$ for 5 min. The color change of the solution in the
183 test tube was then observed. The experiment was repeated three times.

184 The CMC of copolymers was determined by fluorescence spectroscopy using
185 pyrene as fluorescent probe.^{38,39} A series of copolymer solutions were prepared with
186 concentrations varying from 1.0×10^{-3} to 5.0 mg/mL, whereas the concentration of
187 pyrene was fixed at 2.0×10^{-6} M. The excitation spectra of the above solutions were
188 recorded on Perkin Elmer LS55 fluorescence spectrometer at an excitation wavenumber
189 of 390 nm. The CMC value was estimated from the intersection of regression lines of
190 intensity ratio at 339.2 and 336 nm *versus* the logarithm of concentration plots.

191 The hydrodynamic size and zeta potential of copolymer micelles were determined
192 by using Nano-ZS90 nanosizer (Malvern, Worcestershire, UK). Dynamic light
193 scattering (DLS) was performed at 25 $^{\circ}\text{C}$ at a scattering angle of 90 $^{\circ}$. Copolymer
194 solutions at 1.0 mg/mL were filtered through a 0.45 μm cellulose acetate membrane
195 before measurements.

196 The morphology of micelles was observed by TEM on a JEM-1200EX microscope
197 with an acceleration voltage of 80 kV. A copper mesh was immersed in 1.0 mg/mL
198 micelle solution for 1 min and then removed. A small volume of 2.0% phosphotungstic
199 acid solution was dropped at the copper mesh for staining, and air dried at room
200 temperature prior to measurement.

201 **2.5. In vitro drug release**

202 Drug-loaded micelles were prepared in two steps. 20 mg copolymer was first
203 dissolved in 20 mL distilled water to yield blank micelles. 2 mg curcumin dissolved in
204 50 μ L acetone was then added to the micellar solution under vigorous stirring. Drug-
205 loaded micelles were obtained after evaporation of the solvent overnight. Unloaded
206 drug was eliminated by filtration using 0.8 μ m cellulose acetate filter. Finally the
207 solution was lyophilized and stored at 4 $^{\circ}$ C.

208 Lyophilized micelles were dispersed in pH 7.4 phosphate buffered saline (PBS) to
209 prepare a micellar solution at 2.0 mg/mL, and 3 mL micellar solution was placed in a
210 dialysis bag (molecular weight cut-off 3500). The dialysis bag was placed in 30 mL
211 PBS containing 0.5% Tween 80. Drug release studies were performed under constant
212 shaking at 37 $^{\circ}$ C, and the release medium was changed regularly. 35 μ L solution was
213 taken at predetermined time points, and replaced with fresh PBS of the same volume.

214 The drug loading concentration was determined by HPLC. The mobile phase was
215 a mixture of acetonitrile and water 50/50 (v/v). The column temperature was 30 $^{\circ}$ C, and
216 the detection wavelength was 425 nm. 10 μ L of samples were injected for each analysis
217 at a flow rate of 1.0 mL/min. A calibration curve was established from a series of
218 curcumin solutions at concentrations from 0.001 to 0.08 mg/mL. The drug loading
219 content (DLC) and drug loading efficiency (DLE) were calculated from the following
220 formulas :

$$221 \quad \text{DLC (\%)} = \frac{\text{weight of loaded drug}}{\text{weight of polymeric micelles}} \times 100 \quad (1)$$

$$222 \quad \text{DLE (\%)} = \frac{\text{weight of loaded drug}}{\text{therotical drug load}} \times 100 \quad (2)$$

223

224 **2.6. Assay of cytotoxicity of DEX-PLA micelles**

225 Mouse fibroblasts (L-929) were co-cultured with micellar samples to evaluate the
226 cytotoxicity in vitro. After sterilization by exposure to 60 W UV light for 24 h, micellar
227 samples were dispersed in DMEM containing 15% FBS, and then diluted to obtain
228 micellar solutions with final concentrations of 5, 2, 1, 0.5, 0.25 mg/mL, respectively.
229 L929 cells were suspended in DMEM containing 10% FBS, 100 U/mL penicillin and

230 100 µg/mL streptomycin at a concentration of 1×10^4 cells/mL. 100 µL cell suspension
231 was added in each well of a 96-well plate. After that, the medium was incubated for 24
232 h in an environment of 5% CO₂ and 95 % humidity to allow cell adhesion. 100 µL
233 micellar solution was then added to replace the original medium. 100 µL phenol
234 solution at 0.5 mg/mL was used as positive control, and 100 µL fresh medium was used
235 as negative control. After 24, 48 and 72 h, 20 µL MTT solution was added, and cell
236 culture proceeded for 6 h. Finally, all the medium was removed, followed by addition
237 of 150 µL DMSO. The absorbance at 490 nm was measured after gently shaking the
238 solution for 10 min. Cell survival rate or relative activity was calculated as follows:

$$239 \quad \text{Relative activity (\%)} = \frac{\text{OD}_{\text{text sample}}}{\text{OD}_{\text{negative sample}}} \times 100 \quad (3)$$

240

241 **2.7. In vitro antitumor activity**

242 HeLa cells were used to evaluate the antitumor activity of free curcumin and
243 curcumin-loaded micelles by MTT assay. Blank micelles and drug-loaded micelles
244 were dispersed in the medium. Free curcumin dissolved in DMSO was diluted to
245 desired concentrations using the medium. The curcumin concentrations of free drugs
246 and drug loaded micelles ranged from 0.25 to 25 µg/mL. Blank cells served as a
247 negative control. MTT assay was performed using the same protocol described above.
248 The anticancer activity of drug-loaded micelles was evaluated by cell inhibition rate
249 after 48 h. Cell inhibition rate was calculated as follows:

$$250 \quad \text{Cell inhibition rate (\%)} = \frac{\text{OD}_{\text{negative sample}} - \text{OD}_{\text{text sample}}}{\text{OD}_{\text{negative sample}}} \times 100 \quad (4)$$

251

252 **2.8. Statistical analysis**

253 Statistical analysis was carried out by using the sample t-test for in vitro drug
254 release, cytotoxicity of DEX-PLA micelles, and in vitro antitumor activity experiments.
255 All the experiments were performed in triplicates. The data were shown as mean ±
256 standard deviation. Values with $p > 0.05$ were considered not significant, $*p < 0.05$
257 statistically significant, $**p < 0.01$ very significant.

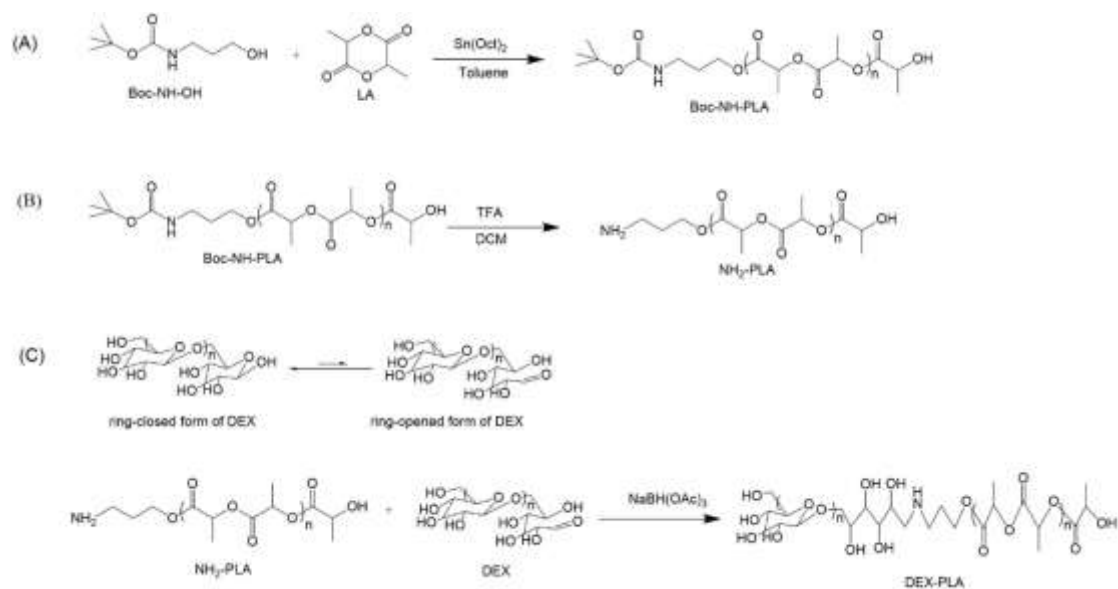
258

259 3. Results and discussion

260 3.1. Synthesis of amphiphilic block copolymers

261 The synthesis of DEX-PLA copolymers was realized in 3 steps according to the
262 method reported by Lu et al.,²⁶ as illustrated in **Scheme 1**. At first, 3-(Boc-amino)-1-
263 propanol was used to initiate the ROP of lactides, yielding Boc-NH-PLA (Scheme 1A).
264 A mixture of L- and DL-lactides with L/DL ratio of 90/10 was used to ensure the
265 solubility of the resulting PLA in DMSO as PLLA with degree of polymerization (DP)
266 above 20 is hardly soluble in DMSO. Then, the protective Boc group at the chain end
267 was removed by treatment using TFA to obtain amino terminated PLA (Scheme 1B).

268



269

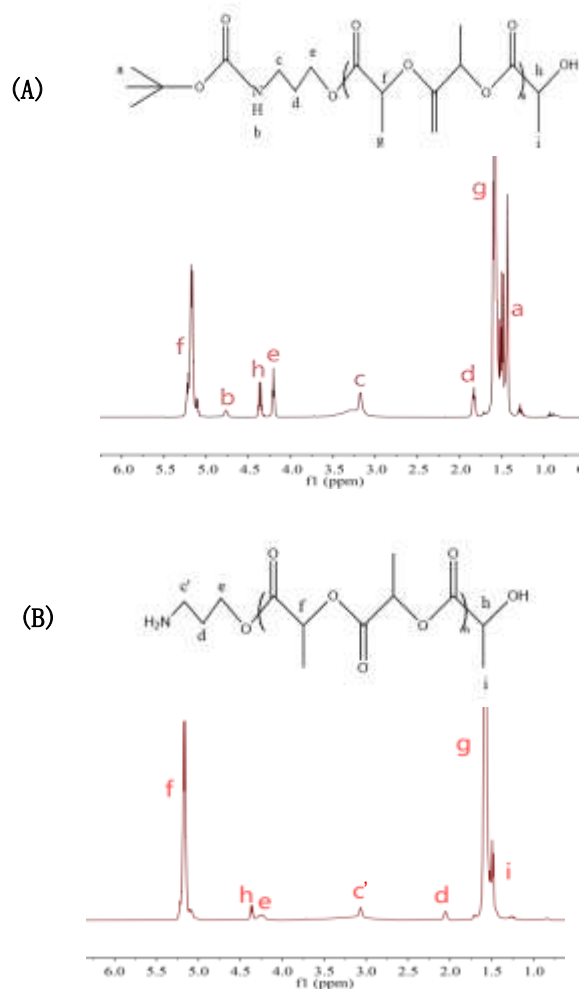
270 Scheme 1. Synthesis route of DEX-PLA block copolymers by reductive amination in three steps:

271 (A) ring opening polymerization; (B) deprotection to remove the protective Boc group; (C)

272 reductive amination.

273

274 It is known that there exists an equilibrium between ring-closed and ring-opened
275 forms in the polysaccharide chain end which is called hemiacetal reducing end, creating
276 an aldehyde group (Scheme 1C). Thus the hemiacetal end group of the hydrophilic DEX
277 block can be conjugated to the amino group of the hydrophobic PLA block in the
278 presence of NaBH(OAc)₃, yielding amphiphilic DEX-PLA block copolymer (Scheme
279 1C).



280

281 Figure 1. ^1H NMR spectra of Boc-NH-PLA (A) and NH_2 -PLA (B) in CDCl_3 .

282

283 Three PLA polymers, namely PLA_{20} , PLA_{30} and PLA_{40} were synthesized in this
 284 work using lactides/3-(Boc-amino)-1-propanol molar ratio of 10/1, 15/1, and 20/1,
 285 respectively. In these abbreviations, the subscript refers to the theoretical DP of PLA.

286 **Figure 1A** shows the ^1H NMR spectrum of Boc-NH-PLA. The signals at 1.60 (g) and
 287 5.19 (f) belong to the methyl and methine groups in the PLA main chain, and the signals
 288 at 1.50 (i) and 4.38 (h) to the methyl group and methine groups of the hydroxyl end of
 289 PLA, respectively. The characteristic methyl signal of Boc group is detected at 1.45 (a),
 290 the NH connected to the Boc group is detected at 4.75 (b), and the three methylene
 291 groups of 3-(Boc-amino)-1-propanol are detected at 3.20 (c), 1.85 (d) and 4.23 (e),
 292 respectively.

293 The DP of Boc-NH-PLA was determined from the integral ratio of signal f and

294 signal h. As shown in **Table 1**, the DP obtained from NMR are close to the theoretical
295 values. The number average molecular weight (M_n) of the three Boc-NH-PLA samples
296 ranges between 1820 and 2900, as calculated from the DP of PLA and the molecular
297 weight of the protective group.

298 GPC was used to determine the molecular weight and dispersity (\mathcal{D}) of the
299 polymers, and the results are shown in **Table 1**. The M_n values obtained from GPC
300 range from 1884 to 3160, which are slightly larger than those obtained from NMR. The
301 dispersity of the polymers is between 1.22 and 1.37, in agreement with narrow
302 molecular weight distribution of the polymers.

303

304 Table 1. Characterization of Boc-NH-PLA polymers

Sample	DP_{NMR}	$M_{n\text{NMR}}$	$M_{n\text{GPC}}$	PD_{GPC}
Boc-NH-PLA ₂₀	23	1820	1880	1.23
Boc-NH-PLA ₃₀	28	2180	2230	1.37
Boc-NH-PLA ₄₀	38	2900	3160	1.22

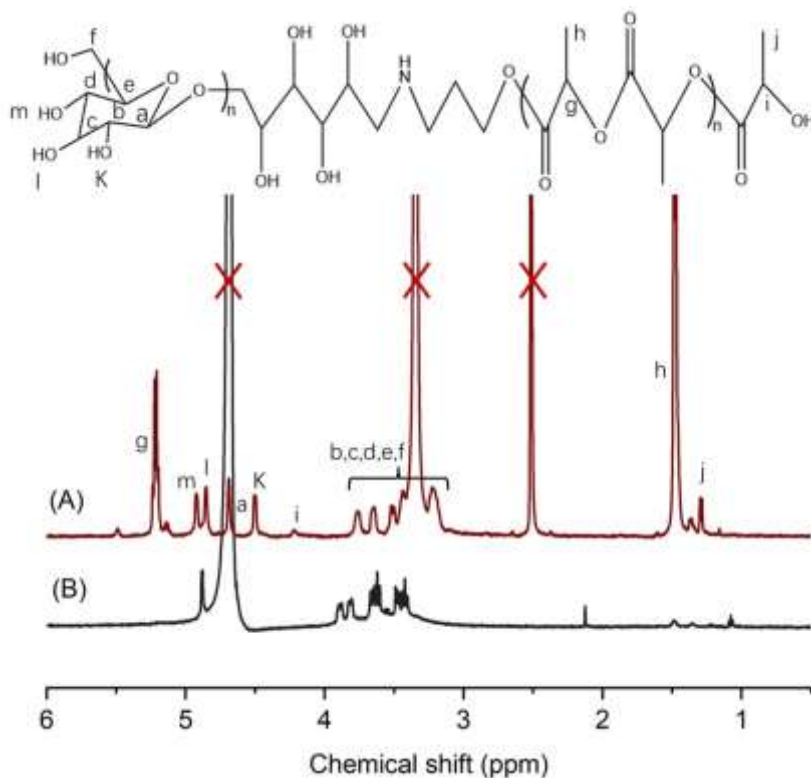
305

306 Amino terminated PLA was obtained by removing the Boc group from Boc-NH-
307 PLA under the action of TFA, as shown in **Figure 1B**. The characteristic methyl signal
308 of the Boc group disappears, and the methylene signal at 3.20 (c) shifts to 3.10 (c') due
309 to the conversion of amide group to amino group. These findings indicate that the
310 deprotection was completed and amino PLA was successfully synthesized.

311 Finally, DEX-PLA block copolymer was obtained by reducing amination of DEX
312 and amino PLA under the action of $\text{NaBH}(\text{OAc})_3$ as reducing agent. The NMR spectra
313 of DEX-PLA polymer in DMSO-d_6 and D_2O are shown in **Figure 2**. The spectrum in
314 DMSO-d_6 shows all the characteristic signals of DEX and PLA, i.e. signals at 1.46 (h)
315 and 5.19 (g) corresponding to the methine and methyl groups of main chain PLA,
316 signals at 1.28 (j) and 4.22 (i) corresponding to the methine and methyl groups of the
317 chain end of PLA, and signals corresponding to the various protons on the glucan ring
318 of DEX (a, b, c, d, e, and f).⁴⁰ Signals belonging to different OH protons are also

319 observed (k, l, m). In contrast, the signals of PLA are not detected on the NMR spectrum
320 of DEX-PLA in D₂O because amphiphilic DEX-PLA block copolymer tends to form
321 micelles in aqueous medium and, in consequence, PLA signals are invisible in NMR as
322 PLA blocks are embedded in the core of micelles. It is also noticed that the signals of
323 OH protons disappear on the NMR spectrum of DEX-PLA in D₂O. On the other hand,
324 the signals of protons on the glucan ring of DEX shifted downfield in D₂O as compared
325 to those in DMSO-d₆. These results indicate that DEX-PLA polymer has been
326 successfully synthesized by reducing amination.

327



328

329 Figure 2. NMR spectra of DEX-PLA in DMSO-d₆ (A) and D₂O (B). The cross symbols indicate

330 peaks of water (3.3 ppm) in Fig. 2A, and the isotopomer with one less deuterium than the

331 perdeuterated molecule, *i.e.* DMSO-d₅ (2.5 ppm) in Fig. 2A, and HDO (4.8 ppm) in Fig. 2B.

332

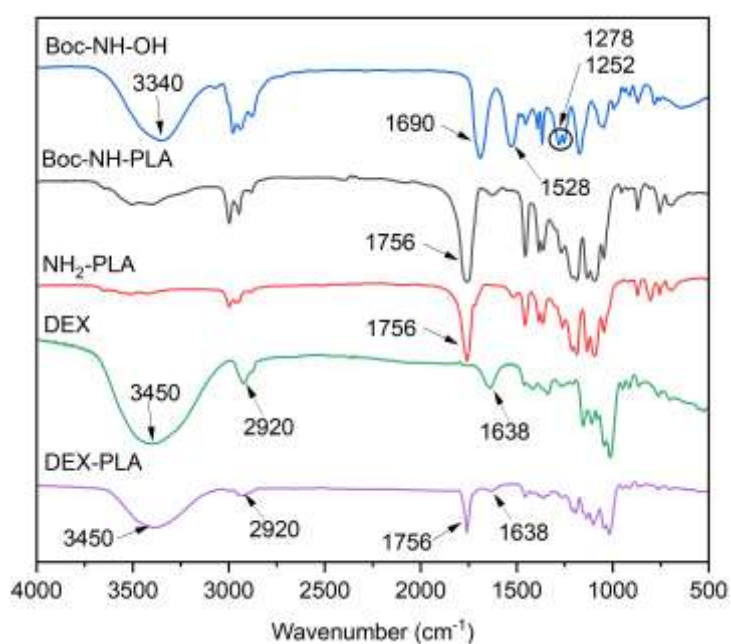
333 FT-IR was also used to analyze the chemical structure of DEX-PLA and its

334 precursors. **Figure 3** shows the FT-IR spectra of 3-(Boc-amino)-1-propanol, Boc-NH-

335 PLA, NH₂-PLA, DEX, and DEX-PLA. 3-(Boc-amino)-1-propanol has a large band at

336 3340 cm^{-1} attributed to hydroxyl groups, and several bands around 3000 cm^{-1} belonging
337 to various methyl and methylene groups. The bands at 1690 and 1528 cm^{-1} are attributed
338 to the carbonyl NH bonds. The bands at 1252 and 1278 cm^{-1} are attributed to the C=O
339 and C-H bonds. On the spectrum of Boc-NH-PLA, an intense band is detected at 1756
340 cm^{-1} , which is assigned to the carbonyl bond of PLA ester groups. After removal of the
341 Boc group, the intensity of several bands near 3000 cm^{-1} is weakened. The spectrum of
342 DEX presents three major bands at 3450, 2920, and 1638 cm^{-1} , which are assigned to
343 hydroxyl groups, C-H bonds, and carbonyl group of the sugar hydrate, respectively. On
344 the spectrum of DEX-PLA, the characteristic bands of both DEX and PLA are observed,
345 especially the hydroxyl band and carboxyl band of DEX at 3450 and 1638 cm^{-1} , and
346 the carbonyl band of PLA at 1756 cm^{-1} , which further proved the successful synthesis
347 of DEX-PLA polymer.

348



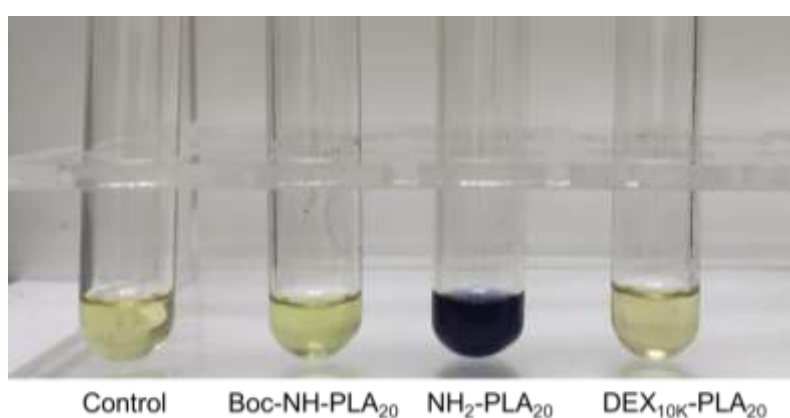
349

350 Figure 3 FT-IR spectra of 3-(Boc-amino)-1-propanol, Boc-NH-PLA, NH_2 -PLA, DEX, and
351 DEX-PLA.

352

353 Kaiser test is commonly used to verify the presence of primary amines since the
354 action of ninhydrin with an amino group will produce a unique bluish purple color. As
355 the main component of the kit, ninhydrin is first dehydrated and condensates with an

356 amino group (ammonia or primary amine) to obtain imines. Then the imines are
357 isomerized into another form of imines after decarboxylation, and hydrolyzed to yield
358 a primary amine and an aldehyde. The primary amine is further condensed with
359 ninhydrin to produce a dimerized imine derivative that appears bluish purple. As shown
360 in **Figure 4**, the color of Boc-NH-PLA and DEX-PLA is yellow, which is the same as
361 that of the control, whereas the color of NH₂-PLA is blue-purple. This finding indicates
362 that the Boc group has been successfully removed and the final polymer has been
363 successfully synthesized, in agreement with NMR data in **Figure 1**.
364



365

366 Figure 4. Kaiser test of Boc-NH-PLA₂₀, NH₂-PLA₂₀ and DEX_{5K}-PLA₂₀

367 **3.2. Self-assembly of copolymers**

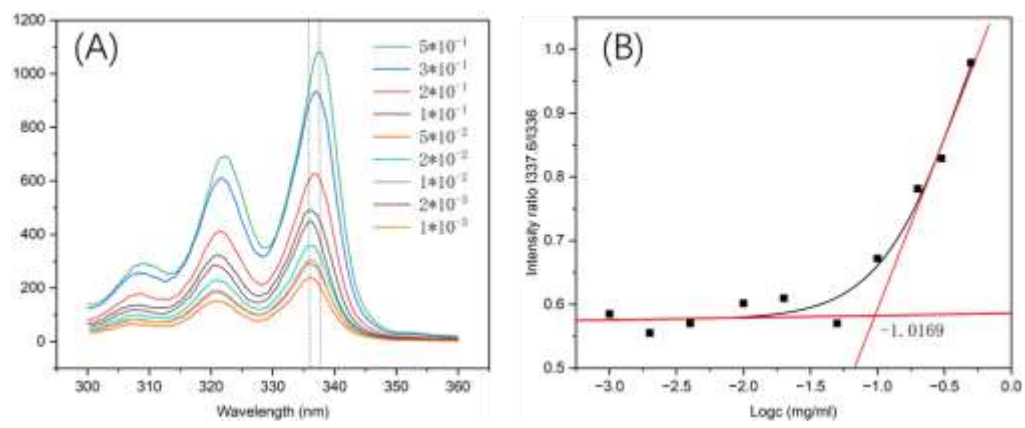
368 DEX-PLA copolymer micelles were prepared by direct dissolution method. The
369 copolymer was dissolved in ultra-pure water. The solution was stirred overnight to
370 achieve self-assembly of the copolymer. The self-assembly properties of copolymers
371 were studied by using fluorescence spectroscopy DLS, and TEM.

372 The CMC is an important parameter of micelles as it reflects the micelle
373 stability.⁴¹⁻⁴³ The lower the CMC, the better the micelle stability. Fluorescence
374 spectroscopy was used to determine the CMC of block copolymers using pyrene as a
375 fluorescence probe. As shown in **Figure 5A**, with the increase of polymer concentration,
376 the fluorescence intensity of pyrene molecules at the same concentration continuously
377 increases, and its maximum excitation wavelength red-shifts from 336.0 nm to 337.6
378 nm. The finding implies that pyrene molecules are transferred from aqueous

379 environment to hydrophobic environment, in agreement with formation of micelles
380 with a hydrophobic core. The fluorescence intensity ratio at 337.6 and 336.0 nm was
381 plotted with the logarithm of copolymer concentration as shown in **Figure 5B**. The
382 CMC was obtained from the intersection point of the regression line.

383 **Table 2** summarizes the CMC values of the six DEX-PLA copolymers. The CMC
384 decreases from 0.0629 mg/mL for DEX_{5K}-PLA₂₀ to 0.0092 mg/mL for DEX_{5K}-PLA₄₀,
385 and from 0.0597 mg/mL for DEX_{10K}-PLA₂₀ to 0.0084 mg/mL for DEX_{10K}-PLA₄₀.
386 Therefore, the longer the hydrophobic block length, the lower the CMC of copolymers.
387 The DEX block seems to have little influence on the CMC.^{44,45}

388



389
390

391 Figure 5. Fluorescence excitation spectra of DEX_{5K}-PLA₂₀ solutions with concentrations varying
392 from 1.0×10^{-3} to 5.0 mg/mL (A), and fluorescence intensity ratio at 337.6 and 336.0 nm
393 ($I_{337.6}/I_{336}$) plotted *versus* the logarithm of copolymer concentration (logC) (B).

394

395 The particle size and polydispersity index (PDI) of micelles were determined by
396 DLS (**Figure 6A**), and the results are summarized in **Table 2**. The micelle size ranges
397 from 208.5 nm of DEX_{5K}-PLA₂₀ to 241.9 nm of DEX_{5K}-PLA₄₀, and from 243.5 nm of
398 DEX_{10K}-PLA₂₀ to 267.5 nm of DEX_{10K}-PLA₄₀. The PDI ranges from 0.104 to 0.174,
399 suggesting a narrow micelle size distribution. It appears that the micelle size increases
400 with increase of both the hydrophilic and hydrophobic block length.^{46,47} The
401 morphology of micelles was observed by TEM. As shown in **Figure 6B**, the micelles
402 are spherical in shape and relatively uniform in size, ranging from 20 to 50 nm. The

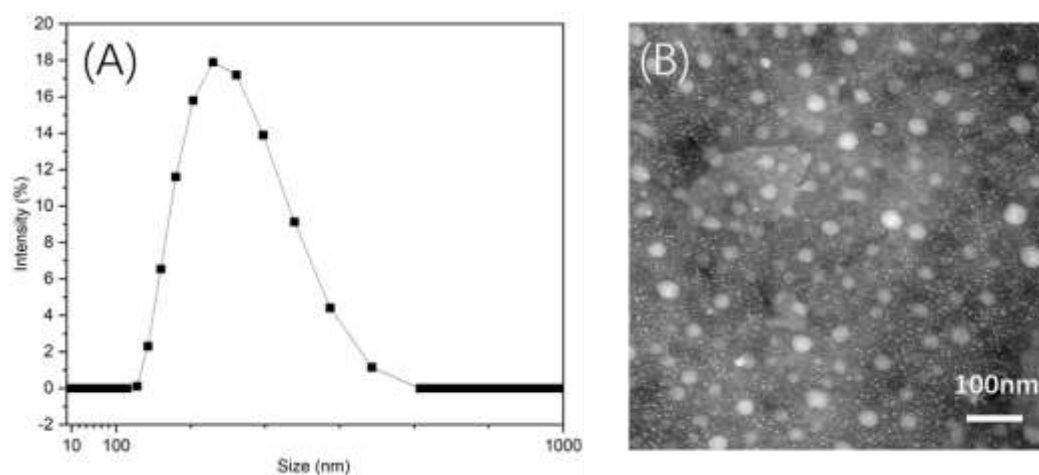
403 micelle size obtained from TEM is much smaller than that obtained from DLS because
 404 of the shrinkage of micelles during air drying before observation by TEM.^{48,49} The zeta
 405 potential of the blank micelle was also determined. It ranges from -6.92 for DEX_{10K}-
 406 PLA₄₀ to -4.67 for DEX_{5K}-PLA₂₀, which is close to zero as the copolymers have no
 407 positive or negative charges.

408

409 Table 2. Size, polydispersity index (PDI), zeta potential and critical micelle concentration (CMC) data
 410 of DEX-PLA block copolymers.

Sample	Blank micelles			
	Size (nm)	PDI	Zeta (mV)	CMC (mg/mL)
DEX _{5K} -PLA ₂₀	208.5±2.9	0.146	-4.67±0.32	0.096
DEX _{5K} -PLA ₃₀	222.9±6.9	0.109	-5.09±0.25	0.0629
DEX _{5K} -PLA ₄₀	241.9±8.8	0.121	-5.86±0.21	0.0092
DEX _{10K} -PLA ₂₀	243.5±0.6	0.104	-5.03±0.15	0.0984
DEX _{10K} -PLA ₃₀	257.8±4.3	0.125	-5.53±0.13	0.0696
DEX _{10K} -PLA ₄₀	265.3±9.9	0.135	-6.92±0.2	0.0103

411



412

413 Figure 6. DLS pattern (A) and TEM image (B) of DEX_{10K}-PLA₄₀ micelles.

414

415 3.3. Drug loading and in vitro drug release

416 Curcumin is a natural polyphenol derived from curcuma longa. It exhibits a wide

417 spectrum of pharmacological activities including anti-oxidant, anti-inflammatory, anti-
 418 microbial, anti-amyloid and anti-tumor properties, and is used for treating inflammation,
 419 cystic fibrosis, Alzheimer's and malarial diseases, and cancer.⁵⁰ However, the
 420 therapeutic efficacy of curcumin is limited by its low water solubility of *c.a.* 11 ng mL⁻¹.⁵¹ In this work, curcumin was used as a model drug to evaluate the drug loading and
 422 release properties of DEX-PLA micelles.

423

424 Table 3. Size, polydispersity index (PDI), zeta potential, DLC and DLE data of drug loaded
 425 micelles prepared from DEX-PLA block copolymers.

Sample	Drug- loading micelles				
	Size (nm)	PDI	Zeta (mV)	DLC (%)	DLE (%)
DEX _{5K} -PLA ₂₀	239.1±5.2	0.111	-2.47±0.27	4.03±0.08	38.7±0.69
DEX _{5K} -PLA ₃₀	240.5±5.5	0.115	-2.94±0.12	4.78±0.4	45.6±3.6
DEX _{5K} -PLA ₄₀	267.3±3.3	0.12	-3.87±0.3	5.44±0.42	51.6±3.73
DEX _{10K} -PLA ₂₀	255.9±2.4	0.104	-2.14±0.21	3.96±0.12	38.1±1.14
DEX _{10K} -PLA ₃₀	272.6±7.6	0.131	-1.81±0.18	4.76±0.39	45.4±3.51
DEX _{10K} -PLA ₄₀	298.8±4.6	0.181	2.17±0.09	5.36±0.1	50.9±3.4

426

427 Drug loaded micelles were prepared by using a two-step method: blank micelles
 428 were first obtained by dissolving DEX-PLA copolymer in distilled water, and a
 429 curcumin solution in acetone was added to the micelle solution under stirring to yield
 430 drug loaded micelles. The particle size, size distribution and zeta potential of micelles
 431 were determined by DLS, as shown in Table 3. The average diameter of drug loaded
 432 micelles ranges from 239.1 nm for DEX_{5K}-PLA₂₀ to 267.3 nm for DEX_{5K}-PLA₄₀, and
 433 from 255.9 nm for DEX_{10K}-PLA₂₀ to 298.8 nm for DEX_{10K}-PLA₄₀. All copolymer
 434 micelles exhibit a low polydispersity (PDI≤0.181). Therefore, the micelle size increases
 435 with increase of DEX and PLA block length as in the case of blank micelles, and the
 436 size of drug loaded micelles is larger than that of blank micelles. On the other hand, the
 437 zeta potential of drug loaded micelles is in the range from -1.81 to 2.17, which is slightly

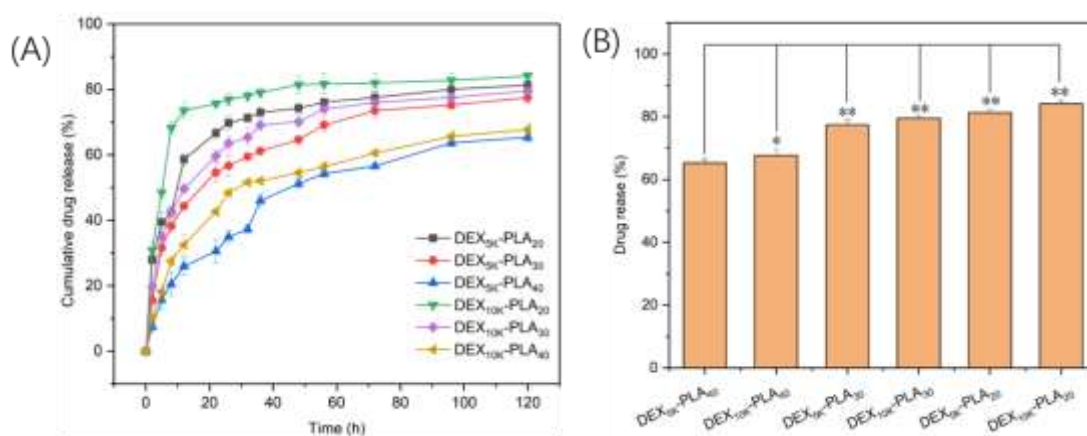
438 higher than that of blank micelles. This increase could be assigned to the fact that
439 curcumin has a positive charge, in agreement with the successfully drug loading in
440 micelles.

441 The performance of drug loading was determined by HPLC. A calibration curve
442 was previously established using a series of curcumin solutions at various
443 concentrations, as shown in **Figure S1**. **Table 3** shows the DLC and DLE data of all
444 drug loaded micelles. The DLC increases from 4.03% for DEX_{5K}-PLA₂₀ to 5.44% for
445 DEX_{5K}-PLA₄₀, and from 3.96% for DEX_{10K}-PLA₂₀ to 5.36% for DEX_{10K}-PLA₄₀. The
446 same trend is observed for DLE data. Therefore, the drug loading capacity of micelles
447 increases with the increase of hydrophobic block length.⁵² In contrast, the hydrophilic
448 block seems to have little effect on drug loading as drug is loaded in the hydrophobic
449 core of micelles.

450 In vitro drug release was performed under in vitro conditions in pH 7.4 PBS at
451 37 °C.⁵³ **Figure 7** shows the drug release profiles on the six drug loaded micelle systems.
452 All micelles present similar drug release characteristics in two stages, namely a burst
453 release in the first 8 h and a slow release up to 120 h. The rapid release in the early stage
454 may be attributed to the release of drug located at the shell-core interface of micelles,
455 whereas the slow release in the late stage results from drug diffusion inside the core of
456 micelles.⁵⁴ At 120 h, the cumulative drug release rate reaches 81.34%, 77.5% and 65.33%
457 for DEX_{5K}-PLA₂₀, DEX_{5K}-PLA₃₀ and DEX_{5K}-PLA₄₀, respectively; and it reaches
458 84.17%, 79.52% and 67.72% for DEX_{10K}-PLA₂₀, DEX_{10K}-PLA₃₀ and DEX_{10K}-PLA₄₀,
459 respectively.

460 It is widely admitted that drug release from biodegradable systems is diffusion
461 and/or degradation controlled.⁵⁵ In the present work, drug release was studied in pH 7.4
462 PBS in a short period of 120 h. The release rate was mainly dependent on drug diffusion
463 as no degradation occurs under these conditions.⁵⁵ Shorter hydrophobic block or higher
464 hydrophilic/hydrophobic ratio led to higher drug release rate as drug diffusion was
465 facilitated. Total drug release was not observed probably because of the slow
466 degradation of the hydrophobic core composed of PLA blocks, in agreement with
467 literature.⁵⁶⁻⁵⁸ Ge et al. reported that Nimodipine-loaded PCL-PEG-PCL micelles

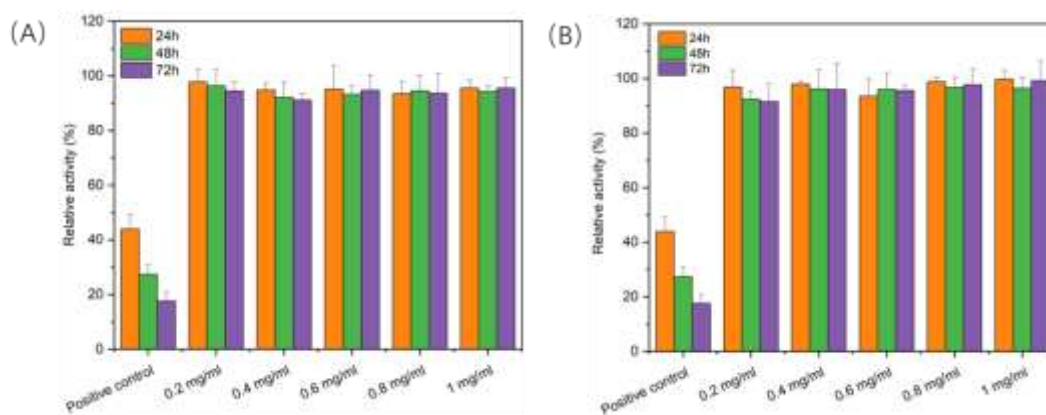
468 present a decrease of drug release rate with increase of PCL block length.⁵⁶ Similarly,
 469 Manjili et al. reported that curcumin release from PCL-PEG micelles decreases from
 470 80.2 to 57.1% with CL/EG ratio increase from 2 to 5.⁵⁷ On the other hand, micelles
 471 with longer hydrophobic block have higher drug load (Table 3). Hu et al. reported that
 472 curcumin loaded P(NIPAAm-co-DMAAm)-b-PLLA copolymer micelles with higher
 473 drug load present slower release rate compared to those with lower drug load.¹⁰ The
 474 authors suggested that curcumin release rate could also depend on the drug loading as
 475 the solubility of curcumin in the release medium could be a limiting factor in cases
 476 where drug release experiments are performed under non sink conditions.
 477



478
 479 Figure 7. In vitro drug release of curcumin from DEX-PLA copolymer micelles. Data are
 480 presented as mean±sd (n = 3, *p < 0.05, **p < 0.01).
 481

482 3.4. Assay of cytotoxicity of DEX-PLA micelles

483 The cytotoxicity of DEX-PLA micelles was evaluated by using MTT method.
 484 **Figure 8** shows the relative activity of L-929 cells after co-culture with solutions of
 485 DEX_{5K}-PLA₂₀ and DEX_{10K}-PLA₂₀ at concentrations from 0.2 to 1.0 mg/mL for 24, 48
 486 and 72 h. The relative activity is above 90% in all cases, even for samples at 1.0 mg/mL
 487 after 72 h culture. Compared with the positive control which has a relative activity of
 488 18% after 72 h culture, the micelles present no cytotoxicity to L-929 cells, indicating
 489 the outstanding biocompatibility of DEX_{5K}-PLA₂₀ and DEX_{10K}-PLA₂₀ micelles.
 490 Similar results were obtained for the 4 other micellar samples.

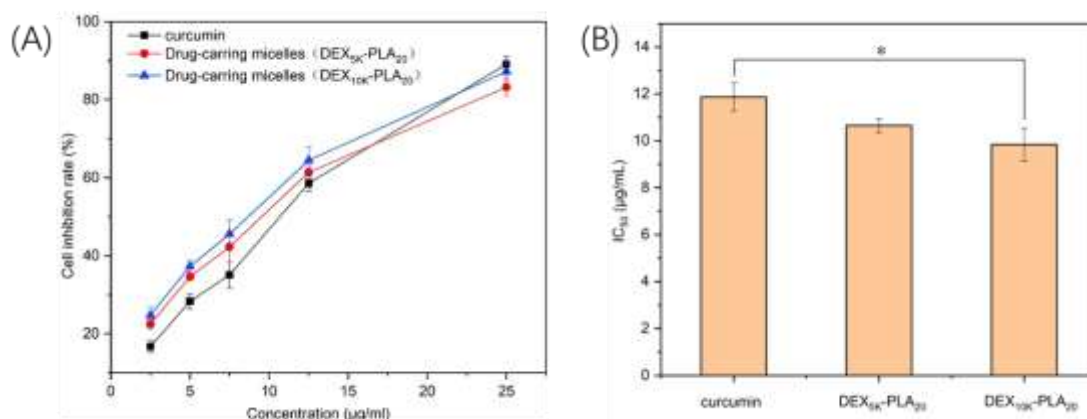


491
 492 Figure 8. Relative activity of L-929 cells after 24, 48 and 72 h culture with DEX_{5K}-PLA₂₀ (A) and
 493 DEX_{10K}-PLA₂₀ (B) micelle solutions at different concentrations in comparison with the positive
 494 control. Data are presented as mean \pm sd (n = 3, p < 0.01).
 495

496 3.5. In vitro antitumor activity

497 The effect of free curcumin and curcumin-loaded micelles on the proliferation of
 498 HeLa cells was examined in the curcumin concentration range of 0.25 to 25 μ g/mL.
 499 **Figure 9A** shows the cell inhibition rate changes as a function of concentration. Free
 500 curcumin and curcumin loaded micelles are highly cytotoxic to HeLa cells, the cell
 501 inhibition rate increasing almost linearly with concentration. The half maximum
 502 inhibitory concentration (IC₅₀) was obtained from data in **Figure 9A**. The IC₅₀ of drug
 503 loaded DEX_{5K}-PLA₂₀ and DEX_{10K}-PLA₂₀ micelles is 10.16 and 9.12 μ g/mL,
 504 respectively, and the IC₅₀ value of free curcumin is 11.9 μ g/mL (**Figure 9B**). Although
 505 these IC₅₀ values are rather close, statistical analysis showed that drug loaded DEX_{10K}-
 506 PLA₂₀ micelles exhibit stronger anticancer effect than free curcumin, which may be
 507 attributed to the more stable nanostructure of micelles and easier endocytosis.^{59,60}
 508 Moreover, drug-loaded micelles can not only increase the drug solubility, but also
 509 reduce the toxic side effects of curcumin on normal tissues.

510



511

512 Figure 9. Inhibition rates (A) and IC₅₀ values (B) of DEX_{5K}-PLA₂₀ and DEX_{10K}-PLA₂₀ drug-loaded
 513 micelles at different concentrations on HeLa cells after 48 h culture, in comparison with free
 514 curcumin. Data are presented as mean±sd (n = 3, *p < 0.05).

515

516 4. Conclusion

517 Amphiphilic DEX-PLA block copolymers with different DEX and PLA block
 518 lengths were synthesized by reduction amination between DEX and amino terminated
 519 PLA. All copolymers can self-assemble into spherical micelles with narrow distribution
 520 in aqueous medium. The CMC of copolymer micelles decreases, and the DLC and DLE
 521 increase with increasing PLA block length. DEX-PLA micelles exhibit biphasic drug
 522 release profiles. The drug release rate depends on the length of the hydrophobic block.
 523 The longer the hydrophobic block, the slower the drug release rate. MTT experiments
 524 showed that DEX-PLA copolymers present good cytocompatibility. Last but not least,
 525 curcumin-loaded micelles exhibit significant cytotoxicity to HeLa cells, suggesting that
 526 DEX-PLA copolymer micelles could be most promising as nanocarrier of hydrophobic
 527 antitumor drugs in cancer treatment.

528

529 CRediT authorship contribution statement

530 **Haozhi Sun and Shuxin Wang:** Methodology, Investigation, Validation,
 531 Formal analysis, Visualization, Writing – original draft; **Yuandou Wang:**
 532 Conceptualization, Methodology; **Linlin Lu:** Funding acquisition, Validation,
 533 Supervision; **Feng Su:** Conceptualization, Supervision, Funding acquisition, Writing -

534 review & editing; **Suming Li**: Conceptualization, Funding acquisition, Supervision,
535 Writing - review & editing.

536

537 **Acknowledgements**

538 The work was financially supported by the Shandong Province Medical and Health
539 Technology Development Plan Project (202203100062) and National Natural Science
540 Foundation of China (32471310), and the Science and technology department of
541 Qingdao Municipality (project number: 24-1-4-xxgg-11-nsh).

542

543 **Data Availability Statement**

544 The data presented in this study are available on request from the corresponding
545 author.

546

547 **Declaration of competing interest**

548 All cited authors certify that they have sufficiently participated in the work to
549 assume public responsibility for the content. The authors declare that there is no
550 conflict of interest regarding the publication of this article.

551

552 **REFERENCES**

- 553 1. Bucholz, T., Sun, Y., Loo, Y.-L. Near-monodispersed polyaniline particles
554 through template synthesis and simultaneous doping with diblock copolymers
555 of PMA and PAAMPSA. *J. Mater. Chem.* 2008; 18:5835-5842.
556 <https://doi.org/10.1039/B810849H>.
- 557 2. Shibata, M., Terashima, T., Koga, T. Thermoresponsive gelation of amphiphilic
558 random copolymer micelles in water. *Macromolecules.* 2021; 54:5241-5248.
559 <https://doi.org/10.1021/acs.macromol.1c00406>.
- 560 3. Liu, Z., Wang, Y., Zhang, N. Micelle-like nanoassemblies based on polymer–
561 drug conjugates as an emerging platform for drug delivery. *Expert Opin. Drug*
562 *Delivery.* 2012; 9:805-822. <https://doi.org/10.1517/17425247.2012.689284>
- 563 4. Ali, I., Kareem, F., Rahim, S., Perveen, S., Ahmed, S., Shah, M. R., Malik, M.
564 I. Architecture based selectivity of Amphiphilic block copolymers of poly
565 (ethylene oxide) and poly (ϵ -caprolactone) for drug delivery. *React. Funct.*
566 *Polym.* 2020; 150:104553.
567 <https://doi.org/10.1016/j.reactfunctpolym.2020.104553>.
- 568 5. Nerantzaki, M., Skoufa, E., Adam, K.-V., Nanaki, S., Avgeropoulos, A.,

- 569 Kostoglou, M., Bikiaris, D. Amphiphilic block copolymer microspheres derived
570 from castor oil, poly (ϵ -caprolactone), and poly (ethylene glycol): Preparation,
571 characterization and application in naltrexone drug delivery. *Materials*. 2018;
572 11:1996. <https://doi.org/10.3390/ma11101996>.
- 573 6. Farhoudi, L., Kesharwani, P., Majeed, M., Johnston, T. P., Sahebkar, A.
574 Polymeric nanomicelles of curcumin: Potential applications in cancer. *Int. J.*
575 *Pharm.* 2022; 617:121622. <https://doi.org/10.1016/j.ijpharm.2022.121622>.
- 576 7. Nguyen, T. B. T., Li, S., Deratani, A. Reverse micelles prepared from
577 amphiphilic polylactide-b-poly (ethylene glycol) block copolymers for
578 controlled release of hydrophilic drugs. *Int. J. Pharm.* 2015; 495:154-161.
579 <https://doi.org/10.1016/j.jconrel.2021.04.014>.
- 580 8. Kaur, J., Mishra, V., Singh, S. K., Gulati, M., Kapoor, B., Chellappan, D. K.,
581 Gupta, G., Dureja, H., Anand, K., Dua, K. Harnessing amphiphilic polymeric
582 micelles for diagnostic and therapeutic applications: Breakthroughs and
583 bottlenecks. *J. Controlled Release*. 2021; 334:64-95.
584 <https://doi.org/10.1016/j.jconrel.2021.04.014>.
- 585 9. Movassaghian, S., Merkel, O. M., Torchilin, V. P. Applications of polymer
586 micelles for imaging and drug delivery. *Wiley Interdiscip. Rev. Nanomed.*
587 *Nanobiotechnol.* 2015; 7:691-707. <https://doi.org/10.1002/wnan.1332>.
- 588 10. Hu, Y., Darcos, V., Monge, S., Li, S., Zhou, Y., Su, F. Thermo-responsive release
589 of curcumin from micelles prepared by self-assembly of amphiphilic
590 P(NIPAAm-co-DMAAm)-b-PLLA-b-P(NIPAAm-co-DMAAm) triblock
591 copolymers. *Int. J. Pharm.* 2014; 476:31-40.
592 <https://doi.org/10.1016/j.ijpharm.2014.09.029>.
- 593 11. Verma, M. S., Liu, S., Chen, Y. Y., Meerasa, A., Gu, F. X. Size-tunable
594 nanoparticles composed of dextran-b-poly (D, L-lactide) for drug delivery
595 applications. *Nano Res.* 2012; 5:49-61. [https://doi.org/10.1007/s12274-011-](https://doi.org/10.1007/s12274-011-0184-z)
596 [0184-z](https://doi.org/10.1007/s12274-011-0184-z).
- 597 12. Wang, H., Han, S., Sun, J., Fan, T., Tian, C., Wu, Y. Preparation of dextran–poly
598 (lactide)–1, 2-dipalmitoyl-sn-glycero-3-phosphoethanolamine copolymer and
599 its micellar characteristics. *Carbohydr. Polym.* 2011; 83:1408-1413.
600 <https://doi.org/10.1016/j.carbpol.2010.10.028>
- 601 13. Wu, J.-h., Hu, T.-g., Wang, H., Zong, M.-h., Wu, H., Wen, P. Electrospinning of
602 PLA nanofibers: Recent advances and its potential application for food
603 packaging. *J. Agric. Food. Chem.* 2022; 70:8207-8221. doi:
604 <https://doi.org/10.1021/acs.jafc.2c02611>.
- 605 14. Gao, H., Fang, X., Chen, H., Qin, Y., Xu, F., Jin, T. Z. Physiochemical properties
606 and food application of antimicrobial PLA film. *Food Control*. 2017; 73:1522-
607 1531. <https://doi.org/10.1016/j.foodcont.2016.11.017>.
- 608 15. Ebrahimi, F., Ramezani Dana, H. Poly lactic acid (PLA) polymers: from
609 properties to biomedical applications. *Int. J. Polym. Mater. Polym. Biomater.*
610 2022; 71:1117-1130. <https://doi.org/10.1080/00914037.2021.1944140>.
- 611 16. Wang, J., Caceres, M., Li, S., Deratani, A. Synthesis and Self-Assembly of
612 Amphiphilic Block Copolymers from Biobased Hydroxypropyl Methyl

- 613 Cellulose and Poly (l-lactide). *Macromol. Chem. Phys.* 2017; 218:1600558.
614 <https://doi.org/10.1002/macp.201600558>.
- 615 17. Rasoulianboroujeni, M., Repp, L., Lee, H. J., Kwon, G. S. Production of
616 paclitaxel-loaded PEG-b-PLA micelles using PEG for drug loading and freeze-
617 drying. *J. Controlled Release.* 2022; 350:350-359.
618 <https://doi.org/10.1016/j.jconrel.2022.08.032>.
- 619 18. Ye, W., Zhu, F., Cai, Y., Wang, L., Zhang, G., Zhao, G., Chu, X., Shuai, Q., Yan,
620 Y. Improved paclitaxel delivery with PEG-b-PLA/zein nanoparticles prepared
621 via flash nanoprecipitation. *Int. J. Biol. Macromol.* 2022; 221:486-495.
622 <https://doi.org/10.1016/j.ijbiomac.2022.09.021>.
- 623 19. Wang, D., Zhou, Y., Li, X., Qu, X., Deng, Y., Wang, Z., He, C., Zou, Y., Jin, Y.,
624 Liu, Y. Mechanisms of pH-sensitivity and cellular internalization of PEOz-b-
625 PLA micelles with varied hydrophilic/hydrophobic ratios and intracellular
626 trafficking routes and fate of the copolymer. *ACS Appl. Mater. Interfaces.* 2017;
627 9:6916-6930. <https://doi.org/10.1021/acsami.6b16376>.
- 628 20. Hu, Y., Darcos, V., Monge, S., Li, S. Synthesis and self-assembling of poly (N-
629 isopropylacrylamide-block-poly (l-lactide)-block - poly (N-
630 isopropylacrylamide) triblock copolymers prepared by combination of ring-
631 opening polymerization and atom transfer radical polymerization. *J. Polym. Sci.,
632 Part A: Polym. Chem.* 2013; 51:3274-3283. <https://doi.org/10.1002/pola.26721>.
- 633 21. Park, K. Impact of Anti-PEG Antibodies on PEGylated Nanoparticles Fate in
634 Vivo. *Journal of Controlled Release* 2018, 287, 257.
635 <https://doi.org/10.1016/j.jconrel.2018.09.014>
- 636 22. Gopinath, V., Saravanan, S., Al-Maleki, A., Ramesh, M., Vadivelu, J. A review
637 of natural polysaccharides for drug delivery applications: Special focus on
638 cellulose, starch and glycogen. *Biomed. Pharmacother.* 2018; 107:96-108.
639 <https://doi.org/10.1016/j.biopha.2018.07.136>.
- 640 23. Plucinski, A., Lyu, Z., Schmidt, B. V. Polysaccharide nanoparticles: From
641 fabrication to applications. *J. Mater. Chem. B.* 2021; 9:7030-7062.
642 <https://doi.org/10.1039/D1TB00628B>.
- 643 24. Liu, J.-Y., Zhang, L.-M. Preparation of a polysaccharide–polyester diblock
644 copolymer and its micellar characteristics. *Carbohydr. Polym.* 2007; 69:196-
645 201. <https://doi.org/10.1016/j.carbpol.2006.09.009>.
- 646 25. Lu, A., Petit, E., Li, S., Wang, Y., Su, F., Monge, S. Novel thermo-responsive
647 micelles prepared from amphiphilic hydroxypropyl methyl cellulose-block-
648 JEFFAMINE copolymers. *Int. J. Biol. Macromol.* 2019; 135:38-45.
649 <https://doi.org/10.1016/j.ijbiomac.2019.05.087>
- 650 26. Lu, A., Petit, E., Jelonek, K., Orchel, A., Kasperczyk, J., Wang, Y., Su, F., Li, S.
651 Self-assembled micelles prepared from bio-based hydroxypropyl methyl
652 cellulose and polylactide amphiphilic block copolymers for anti-tumor drug
653 release. *Int. J. Biol. Macromol.* 2020; 154:39-47.
654 <https://doi.org/10.1016/j.ijbiomac.2020.03.094>.
- 655 27. Lu, A., Petit, E., Wang, Y., Su, F., Li, S. Synthesis and self-assembly of
656 hydroxypropyl methyl cellulose-block-poly (ϵ -caprolactone) copolymers as

- 657 nanocarriers of lipophilic drugs. *ACS Appl. Nano Mater.* 2020; 3:4367-4375.
658 <https://doi.org/10.1021/acsanm.0c00498>.
- 659 28. Varshosaz, J. Dextran conjugates in drug delivery. *Expert Opin. Drug Delivery.*
660 2012; 9:509-523. <https://doi.org/10.1517/17425247.2012.673580>.
- 661 29. Verma M S, Liu S, Chen Y, Y., Meerasa, A., Gu F, X. Size-tunable nanoparticles
662 composed of dextran-b-poly (D, L-lactide) for drug delivery applications. *Nano*
663 *Research.* 2012; 5: 49-61. <https://doi.org/10.1007/s12274-011-0184-z>.
- 664 30. Wang, M., Xu, Y., Wang, J., Liu, M., Yuan, Z., Chen, K., Li, L., Prud'homme,
665 R. K., Guo, X. Biocompatible nanoparticle based on dextran-b-poly (l-lactide)
666 block copolymer formed by flash nanoprecipitation. *Chemistry Letters.* 2015;
667 44:1688-1690. <https://doi.org/10.1246/cl.150800>
- 668 31. Beevers, C. S.,Huang, S. Pharmacological and clinical properties of curcumin.
669 *Botanics: Targets and Therapy.* 2011:5-18.
670 <https://doi.org/10.2147/BTAT.S17244>.
- 671 32. Giordano, A.,Tommonaro, G. Curcumin and cancer. *Nutrients.* 2019; 11:2376.
672 <https://doi.org/10.3390/nu11102376>
- 673 33. Anand, P., Kunnumakkara, A. B., Newman, R. A., Aggarwal, B. B.
674 Bioavailability of curcumin: problems and promises. *Mol. Pharmaceutics.* 2007;
675 4:807-818. <https://dx.doi.org/10.1021/mp700113r>
- 676 34. Lu, A., Petit, E., Wang, Y., Su, F., Li, S. Synthesis and self-assembly of
677 hydroxypropyl methyl cellulose-block-poly (ϵ -caprolactone) copolymers as
678 nanocarriers of lipophilic drugs. *ACS Applied Nano Materials.* 2020, 3(5):
679 4367-4375. <https://dx.doi.org/10.1021/acsanm.0c00498>
- 680 35. Kaiser, E., Colescott, R. L., Bossinger, C. D., Cook, P. Color test for detection
681 of free terminal amino groups in the solid-phase synthesis of peptides. *Anal.*
682 *Biochem.* 1970; 34:595-598. [https://doi.org/10.1016/0003-2697\(70\)90146-6](https://doi.org/10.1016/0003-2697(70)90146-6).
- 683 36. Sarin, V. K., Kent, S. B., Tam, J. P., Merrifield, R. B. Quantitative monitoring
684 of solid-phase peptide synthesis by the ninhydrin reaction. *Anal. Biochem.* 1981;
685 117:147-157. [https://doi.org/10.1016/0003-2697\(81\)90704-1](https://doi.org/10.1016/0003-2697(81)90704-1).
- 686 37. Samori, C., Sainz, R., Ménard-Moyon, C., Toma, F. M., Venturelli, E., Singh,
687 P., Ballestri, M., Prato, M., Bianco, A. Potentiometric titration as a
688 straightforward method to assess the number of functional groups on shortened
689 carbon nanotubes. *Carbon.* 2010; 48:2447-2454.
690 <https://doi.org/10.1016/j.carbon.2010.03.015>.
- 691 38. Chiang, J.-L.,Yang, Y.-W. Modulation of the anticancer activities of paclitaxel
692 by Cremophor micelles. *Int. J. Pharm.* 2021; 603:120699.
693 <https://doi.org/10.1016/j.ijpharm.2021.120699>.
- 694 39. Rezaei, A., Khanzadeh, A., Behniafar, H. PCL-based hydrophobic chains
695 grafted with two PEG-based hydrophilic branches: fluorescence and dynamic
696 light scattering studies. *J. Polym. Res.* 2023; 30:91.
697 <https://doi.org/10.1016/j.nantod.2012.01.002>.
- 698 40. Zhao, Z., Zhang, Z., Chen, L., Cao, Y., He, C., Chen, X. Biodegradable
699 stereocomplex micelles based on dextran-block-poly lactide as efficient drug
700 deliveries. *Langmuir.* 2013; 29:13072-13080.

- 701 <https://doi.org/10.1021/la402890k>.
- 702 41. Yan, J., Ye, Z., Chen, M., Liu, Z., Xiao, Y., Zhang, Y., Zhou, Y., Tan, W., Lang,
703 M. Fine tuning micellar core-forming block of poly (ethylene glycol)-block-
704 poly (ϵ -caprolactone) amphiphilic copolymers based on chemical modification
705 for the solubilization and delivery of doxorubicin. *Biomacromolecules*. 2011;
706 12:2562-2572. <https://doi.org/10.1021/bm200375x>.
- 707 42. Owen, S. C., Chan, D. P., Shoichet, M. S. Polymeric micelle stability. *Nano*
708 *today*. 2012; 7:53-65. <https://doi.org/10.1016/j.nantod.2012.01.002>.
- 709 43. Nakayama, M., Okano, T. Polymer terminal group effects on properties of
710 thermoresponsive polymeric micelles with controlled outer-shell chain lengths.
711 *Biomacromolecules*. 2005; 6:2320-2327. <https://doi.org/10.1021/bm050232w>.
- 712 44. Wang, X., Collot, M., Vandamme, T. F., Anton, N. Study of the spontaneous
713 nano-emulsification process with different octadecyl succinic anhydride
714 derivatives. *Colloids Surf., A*. 2022; 645:128858.
715 <https://doi.org/10.1016/j.colsurfa.2022.128858>.
- 716 45. Abedanzadeh, M., Salmanpour, M., Farjadian, F., Mohammadi, S., Tamaddon,
717 A. M. Curcumin loaded polymeric micelles of variable hydrophobic lengths by
718 RAFT polymerization: Preparation and in-vitro characterization. *J. Drug*
719 *Delivery Sci. Technol.* 2020; 58:101793.
720 <https://doi.org/10.1016/j.jddst.2020.101793>.
- 721 46. Cai, Y., Qi, J., Lu, Y., He, H., Wu, W. The in vivo fate of polymeric micelles.
722 *Adv. Drug Delivery Rev.* 2022; 188:114463.
723 <https://doi.org/10.1016/j.addr.2022.114463>.
- 724 47. Shen, F., Ling, H., Ge, W., Yang, Y., Wang, X., Ren, J., Wang, X. Self-assembly
725 behavior and conformation of amphiphilic hemicellulose-graft-fatty acid
726 micelles. *Carbohydr. Polym.* 2021; 261:117886.
727 <https://doi.org/10.1016/j.carbpol.2021.117886>.
- 728 48. Shen, F., Zhong, H., Ge, W., Ren, J., Wang, X. Quercetin/chitosan-graft-alpha
729 lipoic acid micelles: A versatile antioxidant water dispersion with high stability.
730 *Carbohydr. Polym.* 2020; 234:115927.
731 <https://doi.org/10.1016/j.carbpol.2020.115927>.
- 732 49. Zhao, X., Gong, L., Liao, G., Luan, H., Chen, Q., Liu, D., Feng, Y. Micellar
733 solubilization of petroleum fractions by heavy alkylbenzene sulfonate surfactant.
734 *J. Mol. Liq.* 2021; 329:115519. <https://doi.org/10.1016/j.molliq.2021.115519>.
- 735 50. Tirkey, B., Subuddhi, U. Photophysical Properties, Solubility and Stability of
736 Curcumin in Surfactant Media: The Role of the Surfactant's Head Group. 2022.
737 doi:<http://hdl.handle.net/2080/3721>.
- 738 51. Urošević, M., Nikolić, L., Gajić, I., Nikolić, V., Dinić, A., Miljković, V.
739 Curcumin: Biological activities and modern pharmaceutical forms. *Antibiotics*.
740 2022; 11:135. <https://doi.org/10.3390/antibiotics11020135>.
- 741 52. Zhao, B., Li, L., Lv, X., Du, J., Gu, Z., Li, Z., Cheng, L., Li, C., Hong, Y.
742 Progress and prospects of modified starch-based carriers in anticancer drug
743 delivery. *J. Controlled Release*. 2022; 349:662-678.
744 <https://doi.org/10.1016/j.jconrel.2022.07.024>.

- 745 53. Majumder, N., G Das, N., Das, S. K. Polymeric micelles for anticancer drug
746 delivery. *Therapeutic delivery*. 2020; 11:613-635. [https://doi.org/10.4155/tde-](https://doi.org/10.4155/tde-2020-0008)
747 2020-0008.
- 748 54. Xi, Y., Wang, W., Ma, L., Xu, N., Shi, C., Xu, G., He, H., Pan, W. Alendronate
749 modified mPEG-PLGA nano-micelle drug delivery system loaded with
750 astragaloside has anti-osteoporotic effect in rats. *Drug Delivery*. 2022; 29:2386-
751 2402. <https://doi.org/10.1080/10717544.2022.2086942>.
- 752 55. Jelonek, K., Li, S., Kasperczyk, J., Wu, X.H., Orchel, A. Effect of polymer
753 degradation on prolonged release of paclitaxel from filomicelles of
754 polylactide/poly(ethylene glycol) block copolymers. *Mater Sci Eng C* 2017; 75:
755 918–925. <https://doi.org/10.1016/j.msec.2017.03.006>.
- 756 56. Ge, H., Hu, Y., Jiang, X., Cheng, D., Yuan, Y., Bi, H., Yang, C. Preparation,
757 characterization, and drug release behaviors of drug nimodipine-loaded poly (ϵ -
758 caprolactone)-poly (ethylene oxide)-poly (ϵ -caprolactone) amphiphilic triblock
759 copolymer micelles. *J. Pharm. Sci.* 2002; 91:1463-1473.
760 <https://doi.org/10.1002/jps.10143>.
- 761 57. Manjili, H. K., Ghasemi, P., Malvandi, H., Mousavi, M. S., Attari, E., Danafar,
762 H. Pharmacokinetics and in vivo delivery of curcumin by copolymeric mPEG-
763 PCL micelles. *Eur. J. Pharm. Biopharm.* 2017; 116:17-30.
764 <https://doi.org/10.1016/j.ejpb.2016.10.003>.
- 765 58. Hu, Y., Darcos, V., Monge, S., Li, S., Zhou, Y., Su, F. Thermo-responsive release
766 of curcumin from micelles prepared by self-assembly of amphiphilic P
767 (NIPAAm-co-DMAAm)-b-PLLA-bP (NIPAAm-co-DMAAm) triblock
768 copolymers. *International Journal of Pharmaceutics*. 2014; 476: 31-40.
769 doi:<http://dx.doi.org/10.1016/j.ijpharm.2014.09.029>
- 770 59. Cai, Y., Sun, Z., Fang, X., Fang, X., Xiao, F., Wang, Y., Chen, M. Synthesis,
771 characterization and anti-cancer activity of Pluronic F68–curcumin conjugate
772 micelles. *Drug Delivery*. 2016; 23:2587-2595.
773 <https://doi.org/10.3109/10717544.2015.1037970>.
- 774 60. Zhou, H., Qi, Z., Xue, X., Wang, C. Novel pH-sensitive urushiol-loaded
775 polymeric micelles for enhanced anticancer activity. *Int. J. Nanomed.*
776 2020:3851-3868. <https://doi.org/10.2147/IJN.S250564>.

777

778

779